Miniaturized MIMO-PIFA with Pattern and Polarization Diversity

Soham Ghosh,Thanh-Ngon Tran, and Tho Le-Ngoc
Department of Electrical and Computer Engineering, McGill University
3480 University Street, Montreal, Quebec H3A 2A7, Canada
soham.ghosh@mail.mcgill.ca,ngon.tran@mcgill.ca,tho.le-ngoc@mcgill.ca

***Abstract*—This paper investigates various designs of 4-element miniaturized Planar Inverted-F Antennas (PIFA) with pattern and polarization diversity at 2.45 GHz. The antennas are only 13mm x 7mm in area and built on a small ground plane size of 105 mm x 55 mm. Diversity performance criteria namely the Envelope Correlation Coefficient (ECC) and Mean Effective Gain (MEG) are computed for different fading channel scenarios using the simulated far-field radiation patterns. Then the Effective Diversity Gain (EDG) of all the configurations under the Maximal Ratio Combining (MRC) scheme are generated. The results show that the antenna systems can give a maximum EDG of 16.31 dB as compared to the theoretical limit of 19.12 dB.**

Keywords-PIFA;pattern diversity;polarization diversity;mutual coupling; fading channels;MRC;EDG

I. INTRODUCTION

Multiple-input-multiple-output (MIMO) wireless systems employ multiple antennas at both ends of the communication link and exploit spatial correlation to increase the capacity and diversity. Designing such multi-element antennas (MEA) for small terminals can be a real challenging issue because of the size constraints of mobile devices. Another major problem is the mutual coupling existing between the antenna elements when they are close to each other. The coupling degrades the radiation efficiency severely and increases signal correlation, both of which are detrimental. One way to overcome this problem is to employ pattern or polarization diversity to add extra degrees of freedom (DOF) and make the channels fade in an uncorrelated manner [1]. Various MEA structures have been considered. A 2-element PIFA MEA was designed at 2.5 GHz in [2] but the antenna elements were too big in size. In [3], two spiral PIFAs were proposed but there were no calculations for correlation or diversity gain shown. Other MEA structures like [4] only exploited pattern diversity. 4-element diversity antennas were proposed in [5] but the mutual coupling of -6dB was too high. Compact 4-element antennas were considered in [6] and [7] without investigating their achievable diversity gain in a fading environment. In this paper, we propose very small 4-element PIFA MEA configurations. Even on a small ground plane, they have inter-element mutual coupling less than -10 dB and exploit pattern and polarization diversity. We investigate their characteristics in different fading scenarios and their achievable diversity gain.

The paper is organized as follows: Section II presents the design of the single element. Section III shows the design and characteristics of the various 4-element PIFA configurations. Then Section IV discusses the diversity performance criteria namely ECC, MEG and EDG under MRC. Section V gives the results for the four MEA configurations and finally Section VI concludes the paper.

II. DESIGN OF SINGLE ELEMENT PIFA

The conventional PIFA can be thought of a λ/4 resonator and its structure can be derived from either the monopole or the microstrip patch antenna [8]. It has low profile, good omnidirectional radiation characteristics, wide bandwidth and is quite robust to the influence of other nearby elements making it a good candidate for MIMO systems. The simplest PIFA is usually metallic rectangular patch (LxW) suspended in free-space over height *h* with the coaxial feed and shorting pin at one corner of the patch. The operating frequency for the PIFA can be determined approximately by

$$f_0 = \frac{c}{4(L+W+h)}, \quad \text{c: speed of light} \qquad (1)$$

Here we concentrate on simply meandering the PIFA structure with the objective of increasing the electrical path for miniaturization (Fig.1a-c). It has a small footprint of ~λ/9. At first a single element is simulated on the finite ground plane of size L_g=105 mm and W_g=55 mm near one edge as shown in Fig.1d. A return loss of about -31.6 dB in Fig.2a shows an excellent matching at 2.45GHz. Fig.2b shows the XZ (E-plane) and YZ (H-plane) cuts of the radiation pattern. The pattern is nearly omnidirectional with a peak gain of 3.03 dB and front-to-back-ratio (FTBR) of 11.74 dB. The bandwidth of the antenna is about 60 MHz and a high radiation efficiency of 93.04% is obtained. Designing a PIFA on a finite ground plane

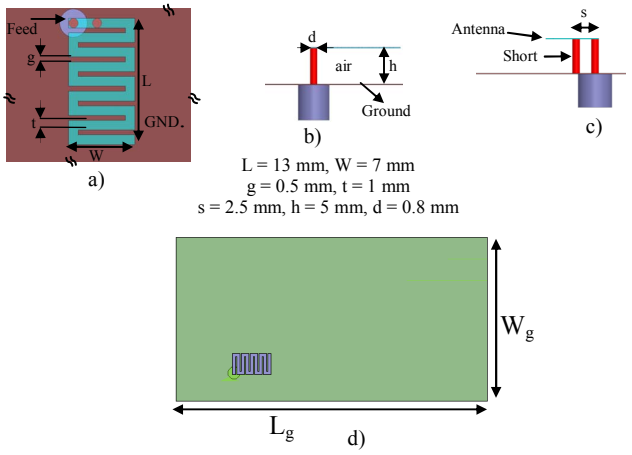

Fig. 1. Single element a) Top view, b) Side view (along L), c) Side view (along W) and d) Location on the ground plane.

978-1-4673-0990-5/12/$31.00 ©2012 IEEE

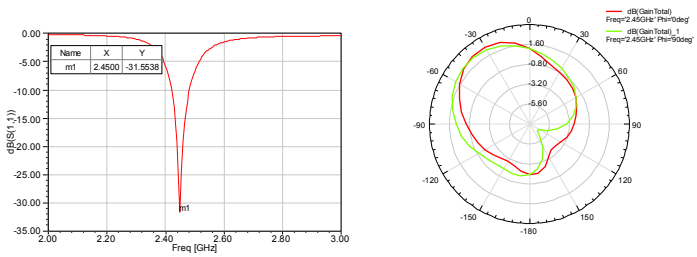

a) b)

Fig. 2. Single element a) Return loss and b) Gain pattern.

has been extensively studied in [9] . They concluded with two optimal PIFA placement strategies. When the ground is rectangular with L_g equal to:

- 0.45λ : the shorting plate of the PIFA should be oriented parallel to the longer edge of the ground plane
- 0.85 λ: the shorting plate should be oriented parallel to the shorter edge of the ground plane.

The second case is the one applicable in our design and here the shorting plate is modified to the form of a pin.

III. MULTI-ELEMENT DESIGN

After tuning the single element, we need to place the other elements in such a way to maximize the diversity performance. It is well known that for antenna spacings of larger than λ, low signal correlations can be obtained and for smaller signal angular spreads even larger spacings are required [10]. But for such small ground planes with spatial constraints we need to consider the following:

- *Complementary nature of radiation patterns*: pattern diversity, reduces the correlation and preserves orthogonality of the signals.
- *Low mutual coupling*: coupling between antennas can be a real determining factor and a low mutual coupling is always beneficial for MIMO systems.
- *Low back lobes:* severe back lobes can reduce the power of the main beam and also increase SAR which is very harmful for the mobile user.
- *Different levels of XPD:* Different levels of XPD between the antenna branches would mean sensitivity to different polarized incoming signals or polarization diversity.

Achieving pattern or polarization diversity inherently depends on the proper placement of the antenna element, feed location

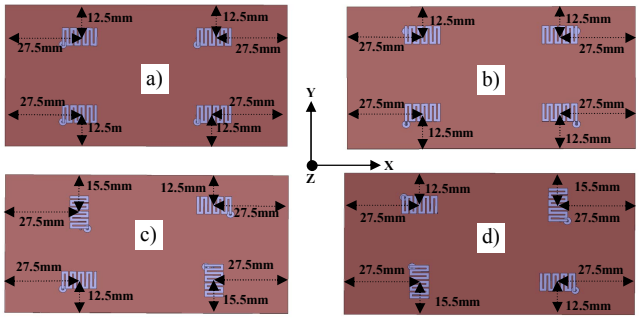

Fig. 3. MEA Configuration: a) One, b) Two, c) Three and d) Four.

TABLE I. INTER-ELEMENT MUTUAL COUPLING

Configuration	S_{21} (dB)	S_{23} (dB)	S_{34} (dB)	S_{41} (dB)	S_{42} (dB)	S_{13} (dB)
1	-11.41	-14.31	-12.31	-14.31	-24	-24
2	-10.24	-12.93	-10.24	-12.93	-19.82	-19.82
3	-11.37	-13.5	-12.49	-13.5	-17	-23.5
4	-12.64	-13.46	-12.64	-13.46	-22.6	-20

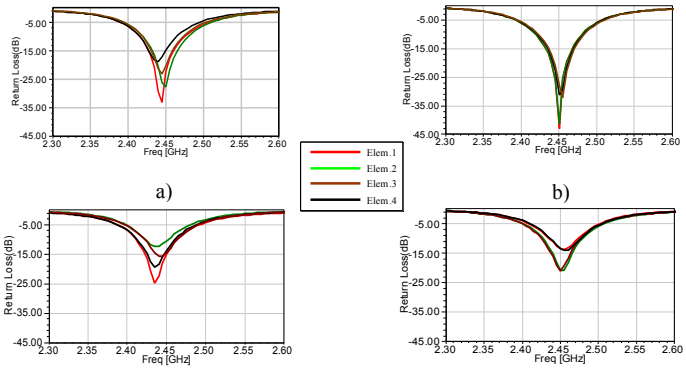

Fig. 4. Return Loss of a) Config.1, b) Config.2, c) Config.3 and d) Config.4.

and orientation. Four different MEA configurations were tried with varying orientations as seen in Fig 3. The placement of the antennas is aimed to keep the mutual coupling as low as possible. Configurations 1 and 2 exploit pattern diversity: Configuration 1 has all the four antennas in the same sense of spatial orientation while in Configuration 2 the feeds are mirror images of each other along the X axis of the ground plane. Configurations 3 and 4 make use of cross-polarized antenna orientation to add polarization diversity on top of pattern diversity. Table I shows the mutual coupling between different antenna branches in the four configurations. Configuration 1 gives the lowest average coupling between the antenna branches followed by Configurations 4, 3 and 2 in the increasing order. Table II summarizes the efficiency of each element in 4 configurations. In Configurations 3 and 4, the elements that are in a cross-polarized fashion suffer some loss in efficiency due to the increased mutual coupling introduced as an effect of proximity to nearby antenna. Figs.4 and 5 show, respectively, the return losses and 3D radiation patterns of the four elements in the four configurations. It is clearly observed in Fig.5 that the radiation pattern of the PIFA elements is complimentary in nature for all the configurations. The polarization diversity of Configurations 3 and 4 is clearly visible in the gain patterns of Fig.6. We see that the G_θ component in elements 2 and 4 of Configuration 3 and elements 1 and 3 of Configuration 4 are much higher than G_Φ.

TABLE II. TOTAL EFFICIENCY (e_{tot}) (%)

Configuration	Elem. 1	Elem. 2	Elem. 3	Elem. 4
1	81.69	79.43	81.59	81.68
2	77.77	77.77	77.69	77.6
3	77.74	67.29	77.49	67.39
4	75.99	81.35	76.36	81.65

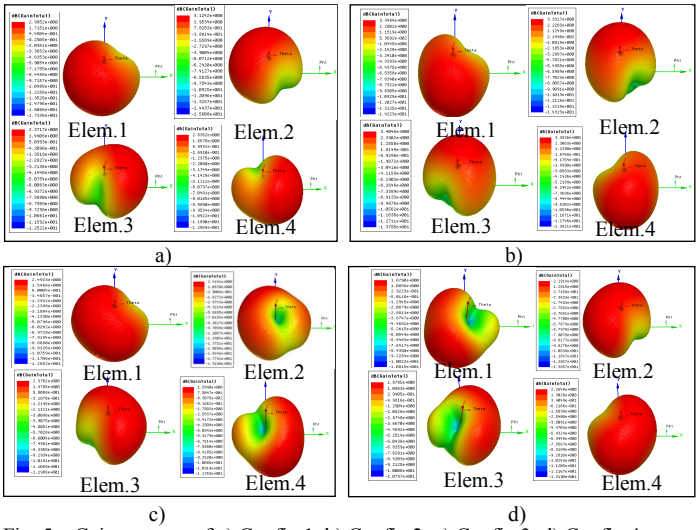

Fig. 5. Gain patterns of a) Config.1, b) Config.2, c) Config.3, d) Config.4.

IV. DIVERSITY PERFORMANCE CRITERIA

A. Correlation

The correlation coefficient of the received signals can be characterized by the Envelope Correlation Coefficient (ECC) in a rich scattering environment [11] as

$$\rho_e \cong |\rho_c|^2 \tag{2}$$

where ρ_c is the complex signal correlation coefficient given by

$$\rho_{c_{ij}} = \frac{\int_0^{2\pi}\int_0^{\pi} A_{ij}(\theta,\phi)\, sin\theta\, d\theta\, d\phi}{\sqrt{\int_0^{2\pi}\int_0^{\pi} A_{ii}(\theta,\phi)\, sin\theta\, d\theta\, d\phi}.\sqrt{\int_0^{2\pi}\int_0^{\pi} A_{jj}(\theta,\phi)\, sin\theta\, d\theta\, d\phi}} \tag{3}$$

$$A_{ij} = XPR.E_{\theta,i}(\theta,\phi)E^*_{\theta,j}(\theta,\phi)P_\theta(\theta,\phi) + E_{\phi,i}(\theta,\phi)E^*{}_{\phi,j}(\theta,\phi)P_\phi(\theta,\phi) \tag{4}$$

$E_{\theta/\Phi}(\theta,\Phi)$ and $P_{\theta/\Phi}(\theta,\Phi)$ are, respectively, the complex electric far-field and the power angular density function of the incoming plane waves in the θ and φ polarizations. XPR is the vertical to horizontal time-average power ratio

$$XPR = \frac{P_v}{P_h} \tag{5}$$

B. Mean Effective Gain

In a multi-path environment the mean effective gain (MEG) defines the power received by the antenna and this property includes antenna radiation power pattern, efficiency and propagation effects. Numerically it is defined as the ratio of the mean received power (P_{rec}) to the mean incident power (P_{inc})[11].

$$MEG_i = \frac{P_{rec}}{P_{inc}} = \int_0^{2\pi}\int_0^{\pi} \frac{XPR.G_{\theta i}(\theta,\phi).P_\theta(\theta,\phi) + G_{\phi i}(\theta,\phi).P_\phi(\theta,\phi)}{1+XPR} sin\theta d\theta d\phi \tag{6}$$

where $G_{\theta i/\Phi i}(\theta,\Phi)$ is the gain pattern of the i-th element. MEG is normalized by a normalization of the gains as

$$\int_0^{2\pi}\int_0^{\pi} \left(G_{\theta i}(\theta,\phi) + G_{\phi i}(\theta,\phi)\right) sin\theta d\theta d\phi = 4\pi.e^i_{tot} \tag{7}$$

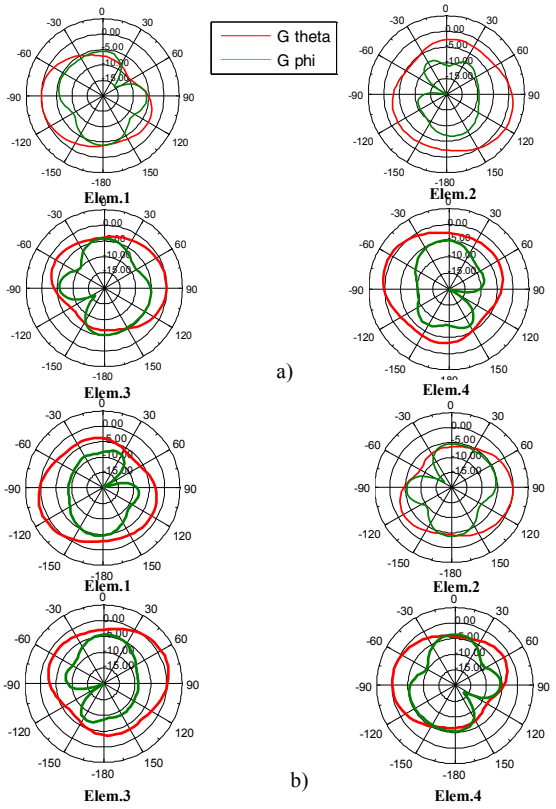

Fig. 6. Gain patterns (XY plane) of a) Config.3 and b) Config.4.

where e^i_{tot} is the total efficiency of the i-th antenna element of the MEA. For good diversity performance, the envelope correlation ρ_e <0.5 and MEG_i/MEG_j ~1, which means that the branch signals are as independent as possible from each other and the power is delivered almost equally to all the branches.

C. Propagation Environment

The correlation and MEG are also related to the distribution of the incoming power and the orientation of the antennas relative to the radio environment. The propagation effects can be quantified by the angular power spectrum of the polarized incoming radio waves. It is important to take into consideration the statistical properties of both the vertical and horizontal polarizations and they can be simplified as [12]

$$P_\theta(\theta,\phi) = P_\theta(\theta).P_\theta(\phi) \tag{8}$$

$$P_\phi(\theta,\phi) = P_\phi(\theta).P_\phi(\phi) \tag{9}$$

where $P_\theta(\theta)$ and $P_\Phi(\theta)$ are the power spectra in elevation and $P_\theta(\varphi)$ and $P_\Phi(\varphi)$ are the power spectra in azimuth. Table III summarizes the four main propagation models under consideration. The mean elevation angles are m_v and m_h and σ_v and σ_h are the standard deviations of the vertical and horizontal wave distributions respectively. A_θ and A_Φ are constants determined by the following conditions

$$\int_0^{2\pi}\int_0^{\pi} P_\theta(\theta,\phi) sin\theta\, d\theta\, d\phi = \int_0^{2\pi}\int_0^{\pi} P_\phi(\theta,\phi) sin\theta\, d\theta\, d\phi = 1 \tag{10}$$

For the indoor environment the incident power spectrum is not uniform. This is because most of the signal energy comes from

TABLE III. PROPAGATION PARAMETERS [12]

Environment	Parameters	
(Uniform/Uniform) Isotropic	$P_\theta(\theta)=\frac{1}{4\pi}, P_\phi(\theta)=\frac{1}{4\pi}, P_\theta(\phi)=1, P_\phi(\phi)=1$	
Gaussian/Uniform	$P_\theta(\theta)=A_\theta.exp\left[-\frac{(\theta-[\pi/2-m_v])^2}{2\sigma_v^2}\right], P_\phi(\theta)=A_\phi.exp\left[-\frac{(\theta-[\pi/2-m_h])^2}{2\sigma_h^2}\right], P_\theta(\phi)=1, P_\phi(\phi)=1$	
	Indoor: XPR= 5 dB, $m_v=10^0$, $m_h=10^0$, $\sigma_v=15^0$, $\sigma_h=15^0$	Outdoor: XPR= 1 dB, $m_v=10^0$, $m_h=10^0$, $\sigma_v=15^0$, $\sigma_h=15^0$
Laplacian/Uniform	$P_\theta(\theta)=A_\theta.\exp\left[-\frac{\sqrt{2}\,\lvert\theta-(\pi/2-m_v)\rvert^2}{\sigma_v}\right], P_\phi(\theta)=A_\phi.\exp\left[-\frac{\sqrt{2}\,\lvert\theta-(\pi/2-m_h)\rvert^2}{\sigma_h}\right], P_\theta(\phi)=1, P_\phi(\phi)=1$	
	Indoor: XPR= 5 dB, $m_v=10^0$, $m_h=10^0$, $\sigma_v=15^0$, $\sigma_h=15^0$	Outdoor: XPR=1 dB, $m_v=20^0$, $m_h=20^0$, $\sigma_v=30^0$, $\sigma_h=30^0$
Elliptical High Directivity	$P_\theta(\theta)=\sqrt{A_\theta}.\frac{S_{\theta\theta}{}^2}{S_{\theta\theta}{}^2+(\sin\theta)^2}, P_\phi(\theta)=\sqrt{A_\phi}.\frac{S_{\phi\theta}{}^2}{S_{\phi\theta}{}^2+(\sin\theta)^2}, P_\theta(\phi)=\sqrt{A_\theta}\alpha_{\theta 0}, P_\phi(\phi)=\sqrt{A_\phi}.(\alpha_{\phi 0}-b_\phi\lvert\phi\rvert)$	
	XPR=5.5 dB, $S_{0,\theta}=0.29$, $S_{\Phi,\theta}=1.06$, $S_{0,\Phi}=0.44$, $S_{\Phi,\Phi}=1.18$, $\alpha_{\theta 0}=0.16$, $\alpha_{\Phi 0}=0.70$, $b_\Phi=0.11$	

the building openings, and for that reason it is more directional with higher XPR. The elliptical distribution model is found to be the best fit for the indoor environment. $a_{\theta 0}$ & $a_{\Phi 0}$ are the relative amplitudes of the uniformly distributed low energy scatterers and b_Φ is the linear decay factor for the horizontal polarized distribution in azimuth. For an isotropic scattering environment, XPR=1 and $P_\theta=P_\Phi=1/4\pi$ and (6) is simplified to

$$MEG_i = \frac{e_{tot}^i}{2} \tag{11}$$

D. Diversity Combining

The signals received by the antenna branches can be combined by additional diversity combining techniques namely Selection Combining (SC), Equal Gain Combining (EGC) and Maximal Ratio Combining (MRC) etc., to increase the mean signal-to-noise ratio (SNR) and to improve the reliability of the link in intense fading environments.

The Effective Diversity Gain (EDG) is defined as the ratio of the SNR obtained by a given diversity combining technique (SNR_{div}) to a reference SNR (SNR_{ref}) obtained by a single ideal antenna subjected to Rayleigh fading. The ratio is taken at a given value of the SNR cumulative probability function (CDF) F(x)=Pr{x<=SNR}[13].

$$EDG = \frac{SNR_{div}}{SNR_{ref}} \tag{12}$$

The CDF of the SNR received by an ideal dual-polarized isotropic antenna branch in Rayleigh fading is given by [11]

$$F_{Rayleigh}(x) = 1 - e^{-\frac{x}{\Gamma}} \tag{13}$$

where Γ is the mean SNR of the branch. In this paper we compare the performance of the four MEA configurations using MRC for all the propagation scenarios of Table III. Assuming a rich scattering environment and non-ideal antennas, the CDF $F_{MRC}(x)$ of the combined SNR can be deduced as[13]

$$F_{MRC}(x) = 1 - \sum_{i=1}^{L} \frac{\lambda_i^{N-1} exp\,(-\frac{x}{\lambda_i})}{\prod_{j\neq i}^{N}(\lambda_i-\lambda_j)} \tag{14}$$

where λ_i's are the eigen values of the signal covariance matrix $\mathbf{\Lambda_{MRC}}$ and L is the number of antenna elements of the MEA. The ij-th element of $\mathbf{\Lambda_{MRC}}$ is related to the complex correlation coefficient ρ_c and MEG's of the antennas i and j as

$$\Lambda_{ij,MRC} = \rho_{cij}\sqrt{MEG_i MEG_j} \tag{15}$$

For an ideal dual-polarized isotropic MEA subjected to i.i.d Rayleigh fading, the CDF of the SNR after MRC (assuming that the average SNR for all branches are equal) is simplified to [14]

$$F_{MRC\ ideal}(x) = 1 - e^{-\frac{x}{\Gamma}}.\sum_{i=1}^{L}\frac{(x/\Gamma)^{i-1}}{(i-1)!} \tag{16}$$

V. Results of the Four MEA Configurations

The far-field radiation patterns of the antennas are generated by HFSS™ and post-processed in MATLAB for different fading channel models of Table III. MEG and ECC results for the four PIFA configurations are shown in Table IV. It is seen that all the configurations satisfy the two main diversity criteria (ρ_e <0.5 and MEG_i/MEG_j ~1). The configuration having the lowest correlation, highest MEG and equal MEG branch ratios is expected to give the best EDG using MRC. On account of the pattern and polarization diversity, very low average ECC in the range of 0.01-0.06 are obtained for the four configurations. The MEG varies with the propagation environment. MEG is higher for outdoor than indoor environments and lowest for the isotropic scattering scenario. The difference in MEG among the antenna elements depend on the symmetry of the configuration. The antenna elements in

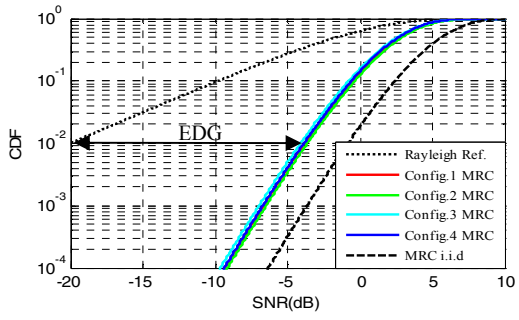

Fig. 7. CDF for MRC in elliptical high directivity environment.

TABLE IV. RESULTS OF THE MEA CONFIGURATIONS

Environment	Configuration 1			Configuration 2			Configuration 3			Configuration 4		
	EDG(dB)	MEG(dB) Avg.	ECC Avg.	EDG(dB)	MEG(dB) Avg.	ECC Avg.	EDG(dB)	MEG(dB) Avg.	ECC Avg.	EDG(dB)	MEG(dB) Avg.	ECC Avg.
Uniform/Uniform (Isotropic)	15.08	-3.92 *Max= -3.89 Min= -4.01*	0.02	14.91	-4.11 *Max:-4.10 Min: -4.11*	0.02	14.62	-4.30 *Max: -4.10 Min:-4.73*	0.03	14.95	-4.05 Max:-3.89 Min:-4.20	0.02
Gaussian/ Uniform (indoor)	16.29	-6.15 *Max:-5.7 Min:-6.57*	0.03	16.15	-6.68 *Max:-6.64 Min:-6.72*	0.01	16.07	-6.23 *Max:-4.89 Min:-7.18*	0.06	16.18	-6.37 *Max:-5.8 Min:-6.93*	0.03
Gaussian/ Uniform (outdoor)	15.65	-7.77 *Max:-7.6 Min:-7.92*	0.02	15.47	-8.24 *Max:-8.19 Min:-8.29*	0.01	15.43	-7.97 *Max:-7.35 Min:-8.36*	0.04	15.49	-8.01 *Max:-7.87 Min:-8.14*	0.02
Laplacian/ Uniform (indoor)	16.31	-6.10 *Max:-5.64 Min:-6.54*	0.03	16.16	-6.65 *Max:-6.61 Min:-6.69*	0.01	16.10	-6.18 *Max:-4.80 Min:-7.15*	0.06	16.21	-6.31 *Max:-5.72 Min:-6.89*	0.03
Laplacian/ Uniform(outdoor)	15.93	-7.1 *Max:-7.05 Min:-7.15*	0.02	15.84	-7.38 *Max:-7.33 Min:-7.44*	0.01	15.58	-7.61 *Max:-7.26 Min:-8.18*	0.04	15.66	-7.64 *Max:-7.14 Min:-8.17*	0.02
Elliptical (High D)	16.15	-7.69 *Max:-7.47 Min:-7.85*	0.03	16.31	-7.42 *Max:-7.24 Min:-7.67*	0.02	15.85	-8.06 *Max:-7.6 Min:-8.49*	0.05	16.09	-8.01 *Max:-7.60 Min:-8.62*	0.01

Configuration 2 have similar MEGs with a balanced feed and symmetrical structure. However in Configurations 3 and 4, the MEGs of the antenna elements are more different. It is observed that the differences in EDG between the four PIFA configurations are only 0.1-0.4 dB. The isotropic scattering environment with XPR= 0 dB gives the least EDG. In the other cases, the EDG for indoor is 0.6 dB greater than outdoor on average. A very high EDG in the range of 14.62-16.31 dB is achieved by the four configurations. In comparison, theoretical MRC using ideal antennas in Rayleigh fading gives an EDG of 19.12 dB. The above mentioned EDG values are taken at SNR CDF of 0.01. Fig.7 shows the CDF of the SNR of the four configurations after MRC in an elliptical environment.

VI. CONCLUSION

Various 4-element miniaturized PIFA configurations were simulated keeping the mutual coupling less than -10 dB for all cases. The configurations were investigated in different fading channel scenarios. It is seen that either pattern diversity or hybrid pattern and polarization diversity can achieve very low signal correlations even in such small ground planes. The four configurations give very similar EDG. So designing antennas for such small form factors, we can just concentrate on maximizing the element efficiency and achieving pattern diversity without caring too much about polarization diversity as it leads to more unequal branch powers. In conclusion, the proposed MEA configurations achieve a maximum effective diversity gain of 16.31 dB which is only 2.81 dB less than the theoretical limit of MRC.

REFERENCES

[1] C. B. Dietrich, Jr., K. Dietze, J. R. Nealy, and W. L. Stutzman, "Spatial, Polarization, and Pattern Diversity for Wireless Handheld Terminals," *IEEE Trans. Antennas Propag.,* vol. 49, no. 9, pp. 1271-1281, Sept. 2001.

[2] G. Yue, C. Xiaodong, Y. Zhinong, and C. Parini, "Design and Performance Investigation of a Dual-Element PIFA Array at 2.5 GHz for MIMO Terminal," *IEEE Trans. Antennas Propag.,* vol. 55, no. 12, pp. 3433-3441, Dec. 2007.

[3] A. T. M. Sayem, S. Khan, and M. Ali, "A Miniature Spiral Diversity Antenna System With High Overall Gain Coverage and Low SAR," *IEEE Antennas Wireless Propag. Lett.,* vol. 8, pp. 49-52, 2009.

[4] R. A. Bhatti, C. Jung-Hwan, and P. Seong-Ook, "Quad-Band MIMO Antenna Array for Portable Wireless Communications Terminals," *IEEE Antennas Wireless Propag. Lett.,* vol. 8, pp. 129-132, 2009.

[5] C. Chi-Yuk and R. D. Murch, "Compact Four-Port Antenna Suitable for Portable MIMO Devices," *IEEE Antennas Wireless Propag. Lett.,* vol. 7, pp. 142-144, 2008.

[6] L. Hui, X. Jiang, and H. Sailing, "A Compact Planar MIMO Antenna System of Four Elements With Similar Radiation Characteristics and Isolation Structure," *IEEE Antennas Wireless Propag. Lett.,* vol. 8, pp. 1107-1110, 2009.

[7] Y. Ding, Z. Du, K. Gong, and Z. Feng, "A Four-Element Antenna System for Mobile Phones," *IEEE Antennas Wireless Propag. Lett.,* vol. 6, pp. 655-658, 2007.

[8] R. Waterhouse, *Printed Antennas for Wireless Communications*. Chichester, UK: Wiley, 2007.

[9] M. C. Huynh and W. Stutzman, "Ground Plane Effects on Planar inverted-F antenna (PIFA) Performance," *Proc. Inst. Elect. Eng. Microw., Antennas Propag.,* vol. 150, no. 4, pp. 209-213, Aug. 2003.

[10] C. Waldschmidt and C. Kuhnert, "On the Integration of MIMO Systems into Handheld Devices," in *Proc. ITG Workshop on Smart Antennas, Munich, Germany,* Mar. 18-19, 2004, pp. 1-8.

[11] K. Fujimoto and J. R. James, *Mobile Antenna Systems Handbook*. Norwood, MA: Artech House, 1994.

[12] V. Plicanic, "Antenna Diversity Studies and Evaluation," *M.S. thesis*, Lund University, Lund, Sweden, 2004.

[13] M. P. Karaboikis, V. C. Papamichael, G. F. Tsachtsiris, C. F. Soras, and V. T. Makios, "Integrating Compact Printed Antennas Onto Small Diversity/MIMO Terminals," *IEEE Trans. Antennas Propag.,* vol. 56, no. 56, pp. 2067-2078, Jul. 2008.

[14] A. Goldsmith, *Wireless Communications*. New York, NY: Cambridge University Press, 2005.